

## Physicochemical properties of commercial starch hydrolyzates in the frozen state

Costas G. Biliaderis<sup>a,\*</sup>, Robert S. Swan<sup>b</sup>, Ioannis Arvanitoyannis<sup>a</sup>

<sup>a</sup>Laboratory of Food Chemistry and Biochemistry, Department of Food Science and Technology, School of Agriculture, Aristotle University, PO Box 256, 540 06 Thessaloniki, Greece

<sup>b</sup>Ault Foods Ltd., 75 Bathurst Street, London, Ontario, Canada N6B 1N8

Received 23 March 1998; received in revised form and accepted 6 July 1998

### Abstract

The physical properties of commercial starch hydrolyzate (varying in dextrose equivalent values, DE, from 0.5 to 42) solutions in the frozen state were related to their composition. At 20% (w/v) hydrolyzate concentration, an inverse linear relationship between DE and apparent glass transition temperature ( $T_g'$ ) of the unfrozen solute matrix was observed. The  $T_g'$  temperatures remained relatively constant for solute concentrations below 40% (w/v); above this concentration the  $T_g'$  was depressed, possibly due to the plasticizing effect of additional water entrapped in the glassy state during non-equilibrium freezing. Simple predictive models (based on the Flory–Fox equation;  $1/T_g = \sum\{w_i/T_{g,i}\}$ ) were found to predict reasonably well the  $T_g'$  value of 'binary' monodisperse and polydisperse hydrolyzate mixtures of varying proportions between the two components. Linear relationships were also found between  $T_g'$  measured (by calorimetry) and  $T_g'$  predicted (based on the Flory–Fox model, and using the oligosaccharide composition of the hydrolyzates and the respective  $T_g'$  values of the pure components). The rate of oxidation of ascorbic acid has been measured in the presence of starch hydrolyzates at temperatures between  $-4$  and  $-16^\circ\text{C}$ . Both the Arrhenius and WLF (Williams–Landel–Ferry) kinetic models were found to describe the temperature dependence of reaction rate constants reasonably well. However, knowing the  $T_g'$  value of the amorphous maltodextrin was not sufficient to predict its cryostabilization behavior. © 1999 Elsevier Science Ltd. All rights reserved.

### 1. Introduction

Starch hydrolyzates (SHs) are widely used in the food industry for a variety of applications. Depending on the starch source, the degree of enzymic- and/or acid-conversion and the conditions employed during hydrolysis, products of different composition are obtained which differ in their physical properties and thus find specific uses. The degree of conversion in SHs, commonly expressed by the dextrose equivalent (DE) value, is a major functionality determinant of these products when used as ingredients in food formulations. Thus, products of low DE, because of their body-imparting properties, are used as thickeners (e.g. exhibiting fat-mimetic properties within a certain DE range), stabilizers and encapsulating carriers (e.g. for frozen items or

spray-dried flavorants). In contrast, products of high DE (glucose syrups) are very hygroscopic with increased sweetness, suitable for beverages, confectionary and bakery products.

During freezing of aqueous solutions mainly two phenomena, of varying intensity, occur depending on the rate and extent of cooling, and the concentration and nature of dissolved solutes: (a) ice crystal formation and (b) vitrification (glass formation) of the freeze-concentrated solute phase. As a physical process, freezing leads to separation of pure ice crystals and a concentrated solute phase (amorphous matrix) which surrounds the ice crystals. The latter phase solidifies as a glassy material at a characteristic temperature,  $T_g$ , where, as a result of very high viscosity ( $\sim 10^{12}$ – $10^{14}$  Pa s<sup>-1</sup>), diffusion and relaxation processes become extremely slow (Slade & Levine, 1991); i.e. at  $T < T_g$ , translational molecular motion of the glass-forming molecules is effectively inhibited. This implies that diffusion-controlled processes (viscous flow, mechanical

\* Corresponding author. Tel.: +30-31-998785; fax: +30-31-998789; e-mail address: biliader@agro.auth.gr.

collapse, diffusion-controlled chemical reactions) cannot be observed on a practical time scale. Above  $T_g$ , freeze-concentrated solutions or complex systems such as foods are in the rubbery or liquid state and therefore are unstable and reactive. The physicochemical properties and 'stability' of a frozen solution can be related to a large extent to its glass transition temperature,  $T_g$  (Levine & Slade, 1986; Slade & Levine, 1991). The glass/rubber transition is a kinetic phenomenon and it depends on the rate of cooling as well as on the type and concentration of solute; e.g. rapidly cooled solutions show lower  $T_g$  values and exhibit less ice at a particular temperature than their slowly cooled counterparts.

A lot of research effort has focused on the formation of glasses in model aqueous systems (Levine & Slade, 1986; Blond, 1989; Blond & Simatos, 1991; Roos & Karel, 1991a–d; Ablett et al., 1992a,b; Roos, 1995). For simplified two-component (solute–water) systems, the phase behavior found in practice is conveniently summarized by a 'state diagram' which represents different states where a system can exist depending on temperature, concentration, time and pressure (Levine & Slade, 1986). More simplified state diagrams, showing the physical state of food materials as a function of concentration and temperature, are convenient means to demonstrate the effect of food composition on material characteristics and stability of amorphous food matrices as well as the effect of different processing protocols on the nature and properties of processed foods (Roos, 1995). In a more simplified state diagram, two curves are mainly shown (i.e. the equilibrium liquidus or ice melting curve, for  $T_m$ , and the kinetically controlled glass-transition curve, for  $T_g$ ) which intersect at a significant point defined by the  $T_g'$  and  $C_g'$  co-ordinates;  $T_g'$  is defined as the glass transition temperature of the maximally freeze-concentrated solute/unfrozen water phase having a solute concentration of  $C_g'$ . These diagrams are usually constructed from measurements carried out by differential scanning calorimetry (DSC). However, there has been some controversy over the interpretation of DSC rewarming traces, as double transitions are often observed, prior to the main ice melting endotherm, for frozen sugar solutions of low solute concentration (Levine & Slade, 1986; Blond, 1989; Roos & Karel, 1991d; Wasyluk & Baust, 1991; Ablett et al., 1992a,b); these multiple glass-like transitions have often been denoted by  $T_g$  and  $T_g'$ , respectively. According to Levine and Slade (1986) and Levine and Slade (1988a), the  $T_g'$  is related to the second (higher temperature) transition, whereas Roos and Karel (1991a, c, d), Izzard et al. (1992a) and Simatos et al. (1989) interpreted this transition as the onset of ice dissolution (melting) that is often denoted by  $T_m'$ . These latter authors have identified the  $T_g'$  for several solutions of sugars at much lower temperatures than the corresponding values given by Slade and Levine (1991). An alternative interpretation

for the two relaxation processes has been forwarded by Shalaev and Franks (1995). These authors have assigned the low and high temperature transitions to a structural glass transition,  $T_g$  (reversible) and a real-time softening process,  $T_s$  or  $T_g'$  (irreversible), respectively. The endothermic effect at  $T_s$  or  $T_g'$  contains contributions from heat absorption due to ice melting and the associated enthalpy changes from the concomitant dilution of the supersaturated solution phase.

Simatos and Blond (1991) have suggested that commencement of ice melting at  $T_g'$ , as reported in the works of Slade and Levine (1991, 1994), may be of critical importance to frozen food stability, particularly in the temperature range of industrial frozen storage. Under common storage conditions, the properties of the unfrozen matrix are such that many of the reactions which result in quality loss in the frozen state may become diffusion-controlled; i.e. mass transport processes are very inefficient and, even for chemical reactions, there is a marked decrease in their rates. In this respect, several arguments have been presented to interpret deviations of reaction kinetics from the Arrhenius formalism in the region of  $T_g' < T < T_m$ . It has thus been suggested that the Williams–Landel–Ferry (WLF) theory is more applicable to describe kinetics in the rubbery domain (Levine & Slade, 1988b; Slade & Levine, 1991). However, this suggestion has been challenged (Simatos et al., 1989).

The main objectives of this study were to further explore: (a) the thermophysical properties of commercial SHs in the frozen state, in relation to their oligosaccharide composition; and (b) the ability of these products to act as protective amorphous matrices for oxidation of ascorbic acid at sub-zero temperatures.

## 2. Materials and methods

### 2.1. Materials

Thirty-five different commercial SHs from corn or potato sources, ranging in DE value from 0.5 to 42, were provided by several suppliers: Staley Manufacturing Co., Decatur, IL (Star-Dri series); American Maize Products Co., Hammond, IN (Amaizo series); Grain Processing Co., Muscatine, IA (Maltrin series); Avebe, Hopelawn, NJ (Avebe series). D-Glucose and D-maltodextrin standards up to and including maltoheptaose were obtained from Boehringer Mannheim GmbH, Germany. Pullulanase (amylopectin 6-glucanohydrolase, EC 3.2.1.41) was purchased from Hayashibara Biochemical Labs., Inc., Okayama, Japan. L-Ascorbic acid was obtained from Fisher Scientific Co., Fair Lawn, NJ.

## 2.2. Oligosaccharide composition of starch hydrolyzates

The compositions of SHs were determined by HPLC using an M-6000A pump, a U6K injector, and a 441 RI detector from Waters. The system was interfaced to a Vista data station (Varian 401) for data acquisition and peak area integration. Native or debranched samples (20 mg ml<sup>-1</sup>, 50 µl injection volume) were run isocratically (85°C), with degassed water at a flow rate of 0.6 ml min<sup>-1</sup>, through an Aminex HPX-42A (300×7.8 mm) column (Bio-Rad Labs, Richmond, CA) in conjunction with a guard column. Column calibration was carried out with standard solutions of glucose oligomers. Prior to sample injection, a standard clean-up procedure was applied by passing the hydrolyzate solution through SEP-PAK C18 cartridge (Waters Associates) and filtering through a 0.45 µm cellulose acetate filter (Millipore Corp., Bedford, MA).

Debranching of the commercial SHs was carried out in 5 ml solutions containing 100 mg carbohydrates with 0.1 ml (40 IU) dialyzed pullulanase preparation in acetate buffer (0.05 M, pH 5.7, 35°C, 24 h). After digestion, the enzyme was inactivated by boiling for 15 min. Aliquots of 1 ml were used for HPLC analysis as described above. The remaining portion of debranched digests was concentrated (~10×) in a Fisher isothermure dry bath and kept for DSC analysis.

## 2.3. Differential scanning calorimetry

All DSC measurements were performed with a DuPont 9900 thermal analyzer equipped with a 910 DuPont cell base and a DSC ambient pressure cell. The analyzer was calibrated for heat flow and temperature using indium ( $T_m$  156.6°C,  $\Delta H_m$  28.5 J g<sup>-1</sup>) and gallium ( $T_m$  29.8°C,  $\Delta H_m$  79.3 J g<sup>-1</sup>). Solutions of ~10–15 mg (20% w/w SH in distilled water) were hermetically sealed in Al-coated DSC pans and scanned at a heating rate of 10°C min<sup>-1</sup> from ca. -70 to 30°C after initial cooling of the samples below -70°C (at ~25–30°C min<sup>-1</sup> cooling rate) with liquid N<sub>2</sub>. At least triplicate scans were made for each sample and the data were recorded as heat flow in mW mg<sup>-1</sup> at 1.0 s<sup>-1</sup> time intervals. The analogue derivative function of the analyzer permitted a more accurate definition of the  $T_g'$  using the terminology proposed in Levine and Slade's work (Fig. 1). Although a second less well-defined glass transition, preceding the  $T_g'$ , was also observed in some of the thermal scans, its appearance was not clear for the intermediate and low DE products under the conditions employed for cooling and heating the SHs solutions at 20% w/v. Therefore, the Levine and Slade's  $T_g'$  was used as the reference point for property evaluation purposes.

A prediction model for  $T_g'$  determination of the SHs (21 samples of native and debranched hydrolyzates), based on their oligosaccharide composition (as

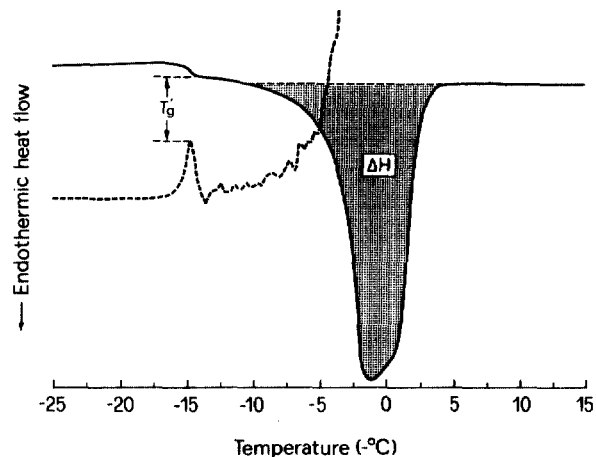


Fig. 1. Typical DSC thermal curve and its first derivative for an aqueous starch hydrolysate at 20% (w/v) showing the  $T_g'$  (defined according to Levine and Slade, 1988c); heating rate 10°C min<sup>-1</sup>.

determined by HPLC) and the respective  $T_g'$  values of pure malto-oligosaccharide standards (glucose to maltoheptaose), was developed by employing a generalized form of the Flory–Fox equation (Fox and Flory, 1954):

$$\frac{1}{T_g} = \sum_{i=0}^{i=n} \left( \frac{w_i}{T_{g_i}} \right)$$

where  $w_i$  and  $T_{g_i}$  are the weight fractions and the glass transition temperature of the  $i$ th constituent in the mixture.

## 2.4. Kinetics of ascorbic acid oxidation in frozen SHs

The rate of oxidation of L-ascorbic acid (AA) to dehydroascorbic acid was examined in initially degassed SHs solutions (20 and 40% w/v in 0.02 M acetate buffer, pH 5.5). L-Ascorbic acid was included in a concentration of 2.5 mg/100 ml and a large amount of H<sub>2</sub>O<sub>2</sub> (1500 ppm) was also added to the reaction mixture. Aliquots (1 ml) of the solutions were quickly frozen in liquid N<sub>2</sub> and then stored at various sub-freezing temperatures (-4, -8, -12, and -16°C). After storage, the tubes were thawed and further oxidation was prevented by the addition of 0.01 N sulfuric acid. The rate of oxidation was monitored by absorbance measurements (residual AA) at 265 nm (Racker, 1952) and the rate constants ( $k$ ) were determined assuming a first-order reaction model.

The temperature dependence of reaction rate constants was examined with the Arrhenius model:

$$k = A.e^{(-E_a/RT)}$$

or

$$\ln k = \ln A - E_a/RT$$

where  $A$  is the frequency factor and  $E_a$  is the activation energy.

Alternatively, the WLF equation (Williams et al., 1955) was employed to analyze temperature effects on reaction rate constants:

$$\log\left(\frac{k}{k_{\text{ref}}}\right) = \frac{-17.44(T - T_{\text{ref}})}{51.6 + (T - T_{\text{ref}})}$$

where  $T$  is the storage temperature,  $T_{\text{ref}}$  is a reference temperature (e.g. the glass transition temperature), and  $k$  and  $k_{\text{ref}}$  are the corresponding rate constants at these temperatures. According to this model, in the rubbery domain ( $T_g < T < T_m$ ), the rates of relaxation processes correlate with the temperature difference  $T - T_{\text{ref}}$ .

### 3. Results and discussion

#### 3.1. Compositional effects on low temperature thermal properties of SH solutions

The thermal curves of the freeze-concentrated SH solutions (20% w/v) were dominated by the ice melting endotherm (Fig. 1). Prior to ice melting, a shift in heat capacity, manifested by a peak on the derivative trace (denoted as  $T_g'$ ) was observed in all cases. For the pure malto-oligosaccharides and some high DE products, in addition to this transition there was also evidence for a second glass transition,  $T_g$  (showing much weaker response on the heat capacity and the first derivative curves than that at  $T_g'$ ), at lower temperatures than the respective  $T_g'$ . However, this was not noticeable for most of the low and intermediate DE hydrolyzates, presumably because of their heterogeneity. For simple sugar solutions such sub- $T_g'$  thermal events, involving a detectable change in heat capacity, have been clearly shown in DSC traces of quickly frozen samples (Levine & Slade, 1986, 1988c; Blond, 1989; Roos & Karel, 1991a, d; Ablett et al., 1992a,b). Moreover, a divitrification exotherm could be observed above the  $T_g$  depending on solute concentration, thermal history of the frozen sample and warming rate. Because of the non-equilibrium nature of the glassy state, as opposed to the crystalline state, a glass permits structural relaxation to occur depending on storage temperature and time. Thus, the manifestation of both  $T_g$  and  $T_g'$  in a DSC trace would depend on solute type and concentration as well as on the cooling rate and any annealing protocol employed before the sample is heated.

The apparent  $T_g'$  values for the glucose and malto-oligosaccharides (20% w/v) solutions showed an inverse relationship with the molecular weight (MW) of the solute:  $T_g' \text{ (K)} = 277.2 - 0.28 \text{ (MW)}^{-1}$ ,  $r^2 = 0.98$

( $p < 0.001$ ). This relationship confirms the findings of Levine and Slade (1988c), and is expected for homologous series of non-entangling monodisperse oligomers (Ferry, 1980). A linear relationship between  $T_g^{-1}$  and the reciprocal degree of polymerization (DP) for dry amorphous glucose and linear malto-oligosaccharides was also reported (Orford et al., 1989); extrapolation of this relationship to large molecular size provided estimates of  $T_g$  for dry amylose and amylopectin ( $\sim 500 \pm 10$  K). In general, the molecular weight dependence of  $T_g$  follows the Fox and Flory (1950) equation:  $T_g = T_g^\infty - K \text{ (MW)}^{-1}$ , where  $T_g^\infty$  is the limiting glass transition of the polymer at the infinite high molecular weight plateau, and  $K$  is a constant characteristic of the polymer. The increase in  $T_g$  with the molecular weight levels off at high MW due to entanglement coupling of the polymer chains (Mansfield, 1993). A  $\text{DP}_n \approx 175$  has been estimated as the critical chain entanglement threshold for substituted amyloses (Bizot et al., 1997), whereas Slade and Levine (1994) claimed a much lower boundary of the entanglement plateau for hydrolyzed starch molecules of about DP 18. The validity of the above relationship was further proven for dry commercial maltodextrins by To and Flink (1978) with measurements of 'collapse' temperatures in freeze-dried samples.

For the frozen aqueous solutions of commercial SHs, the results (Table 1) also showed an inverse linear relationship between apparent  $T_g'$  and DE (inversely related to the DP of starch chains) (Fig. 2), in agreement with the data reported by Levine and Slade (1988c) for another series of commercial hydrolyzates and monodisperse sugars and polyols. In general, for the higher DE products (DE  $\approx 35$ –42), the  $T_g'$  values at any given DE were similar among samples of different origin; a difference of no greater than 0.9 K was found among samples of identical DE value. Conversely, for the low

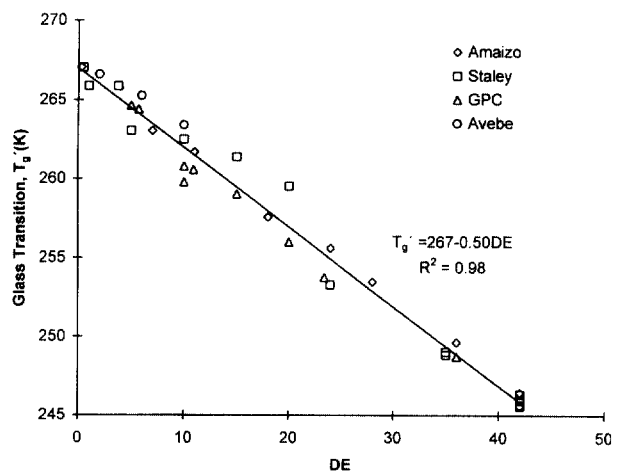


Fig. 2. Relationship between DE and  $T_g'$  of aqueous commercial starch hydrolyzates at 20% (w/v).

Table 1  
Oligosaccharide<sup>a</sup> composition of various commercial starch hydrolysates<sup>b</sup>

Sample	DE <sup>c</sup>	$T_g'(K)$	Composition (%)							$> G_7^e$
			$G_1^d$ ( $T_g' = 229.7$ $\pm 1.1$ )	$G_2$ ( $T_g' = 242.2$ $\pm 0.4$ )	$G_3$ ( $T_g' = 249.1$ $\pm 0.1$ )	$G_4$ ( $T_g' = 252.6$ $\pm 0.2$ )	$G_5$ ( $T_g' = 255.0$ $\pm 0.1$ )	$G_6$ ( $T_g' = 256.0$ $\pm 0.1$ )	$G_7$ ( $T_g' = 259.6$ $\pm 0.1$ )	
Amaizo 42	42	245.6 ± 0.3	19.5 ± 0.33	13.3 ± 0.20	10.4 ± 0.19	8.45 ± 0.18	7.11 ± 0.19	6.05 ± 0.05	4.67 ± 0.13	30.6
Star-Dri 42F	42	245.6 ± 0.2	21.1 ± 0.36	15.5 ± 0.28	12.3 ± 0.22	10.2 ± 0.26	8.61 ± 0.23	6.68 ± 0.15	5.24 ± 0.28	20.3
Amaizo 36	36	249.6 ± 0.1	14.4 ± 0.52	10.3 ± 0.38	8.38 ± 0.33	7.16 ± 0.25	6.31 ± 0.29	5.42 ± 0.10	4.29 ± 0.20	43.8
Maltrin M365	36	248.7 ± 0.1	6.52 ± 0.20	27.9 ± 0.35	16.8 ± 0.19	6.84 ± 0.07	5.01 ± 0.06	4.36 ± 0.14	3.44 ± 0.10	29.2
Star-Dri 35R	35	248.8 ± 0.0	14.3 ± 0.05	11.5 ± 0.05	9.97 ± 0.03	8.66 ± 0.04	7.76 ± 0.04	6.74 ± 0.07	5.43 ± 0.02	35.7
Amaizo 24D	28	253.5 ± 0.1	9.22 ± 0.40	7.47 ± 0.29	6.79 ± 0.23	6.28 ± 0.23	5.77 ± 0.29	5.24 ± 0.25	4.47 ± 0.07	54.8
Amaizo 24-924	24	255.6 ± 0.0	6.31 ± 0.23	5.57 ± 0.19	5.34 ± 0.19	5.24 ± 0.13	5.15 ± 0.16	4.65 ± 0.07	4.04 ± 0.19	63.7
Star-Dri 24R	24	253.3 ± 0.1	6.71 ± 0.09	7.18 ± 0.02	8.23 ± 0.05	7.20 ± 0.10	6.78 ± 0.02	8.69 ± 0.13	8.54 ± 0.05	46.7
Maltrin M250	23.4	253.8 ± 0.0	7.52 ± 0.10	7.20 ± 0.10	7.04 ± 0.11	6.89 ± 0.07	6.67 ± 0.11	5.96 ± 0.12	5.05 ± 0.02	53.7
Maltrin M200	20	255.0 ± 0.0	2.46 ± 0.15	7.99 ± 0.10	9.32 ± 0.11	6.84 ± 0.15	6.65 ± 0.12	13.8 ± 0.25	12.6 ± 0.26	40.3
Star-Dri 20	20	259.5 ± 0.1	2.10 ± 0.02	7.17 ± 0.09	8.33 ± 0.09	5.34 ± 0.08	6.06 ± 0.09	14.9 ± 0.18	10.4 ± 0.15	45.7
Amaizo 15	18	257.6 ± 0.1	4.98 ± 0.17	4.88 ± 0.16	4.92 ± 0.17	5.02 ± 0.18	5.06 ± 0.18	4.65 ± 0.21	4.17 ± 0.05	66.3
Maltrin M150	15	259.0 ± 0.1	0.98 ± 0.18	4.20 ± 0.13	5.87 ± 0.07	4.89 ± 0.06	4.24 ± 0.13	8.62 ± 0.18	–	71.2
Star-Dri 15	15	261.4 ± 0.2	1.25 ± 0.05	3.92 ± 0.05	5.65 ± 0.06	4.11 ± 0.04	3.63 ± 0.08	8.92 ± 0.11	12.4 ± 0.11	59.7
Amaizo 10	11	261.7 ± 0.4	0.70 ± 0.09	2.77 ± 0.14	3.88 ± 0.07	3.20 ± 0.02	2.67 ± 0.07	5.56 ± 0.07	6.55 ± 0.09	74.7
Maltrin M100	10.9	260.5 ± 0.3	0.99 ± 0.22	3.07 ± 0.22	4.51 ± 0.15	3.86 ± 0.10	3.38 ± 0.14	6.28 ± 0.11	7.70 ± 0.28	70.2
Maltrin M500	10	259.8 ± 0.7	0.60 ± 0.04	2.51 ± 0.08	3.99 ± 0.06	3.45 ± 0.04	3.14 ± 0.04	5.50 ± 0.09	6.84 ± 0.10	74.3
Star-Dri 10	10	262.5 ± 0.0	0.85 ± 0.06	1.89 ± 0.10	3.13 ± 0.05	2.48 ± 0.06	2.45 ± 0.09	4.78 ± 0.15	6.01 ± 0.02	78.4
Maltrin M050	5.7	264.4 ± 0.1	0.66 ± 0.12	0.83 ± 0.11	1.03 ± 0.06	1.19 ± 0.08	1.05 ± 0.33	1.48 ± 0.03	1.49 ± 0.01	92.3
Amaizo 5	7	363.0 ± 0.2	0.39 ± 0.02	1.65 ± 0.01	2.72 ± 0.02	2.14 ± 0.02	1.86 ± 0.11	4.26 ± 0.05	5.72 ± 0.01	81.3
Star-Dri 5	5	263.0 ± 0.2	1.07 ± 0.15	1.62 ± 0.03	1.98 ± 0.13	1.59 ± 0.08	1.76 ± 0.12	2.68 ± 0.03	2.31 ± 0.16	87.0
Maltrin M040	5	264.6 ± 0.1	–	0.54 ± 0.18	1.04 ± 0.15	0.99 ± 0.07	1.06 ± 0.15	1.56 ± 0.04	1.92 ± 0.13	92.9
Avebe 10	10	263.4 ± 0.1	–	1.59 ± 0.07	2.96 ± 0.02	2.29 ± 0.04	1.96 ± 0.03	3.95 ± 0.01	5.68 ± 0.03	81.6
Avebe 6	6	265.3 ± 0.1	–	0.94 ± 0.08	1.65 ± 0.02	1.25 ± 0.01	1.06 ± 0.07	2.24 ± 0.07	3.05 ± 0.21	89.8

<sup>a</sup> Data are expressed as per cent of total carbohydrate content (% ± SD,  $n = 3$ ).

<sup>b</sup> From HPLC analysis of starch hydrolysates.

<sup>c</sup> Dextrose equivalent values.

<sup>d</sup> G1–G7 correspond to glucose and malto-oligosaccharides up to maltoheptaose; numbers in parentheses correspond to  $T_g'$  of the pure oligosaccharides.

<sup>e</sup> Determined by difference:  $100 - \Sigma(G_i)$ .

DE products, differences in  $T_g'$  were much greater; e.g. the Star-Dri 15 and Maltrin M150 products had a difference of 2.36 K. These differences may be attributed to the different raw materials and the conversion processes used by various manufacturers in the production of hydrolysates. As a result, the molecular polydispersity and the degree of branching may vary from product to product, and this would reflect on the apparent  $T_g'$  value. For example, a polydisperse SH is more likely to undergo chain entanglement (leading to a higher  $T_g'$ ) than a corresponding monodisperse carbohydrate sample of identical DE, as the former comprises both long and short chains. Indeed, the malto-oligosaccharide standards were consistently found to have  $T_g'$  values of ~2–10 K lower than the respective commercial SHs of comparable DE. The relationship of Fig. 2 also provides a convenient means for predicting the apparent  $T_g'$  of an unknown SH from its DE value.

Determination of  $T_g'$  for SH solutions of different carbohydrate concentration was also carried out, and the results are summarized in Fig. 3. Based on a constant cooling protocol, no annealing effects, and a con-

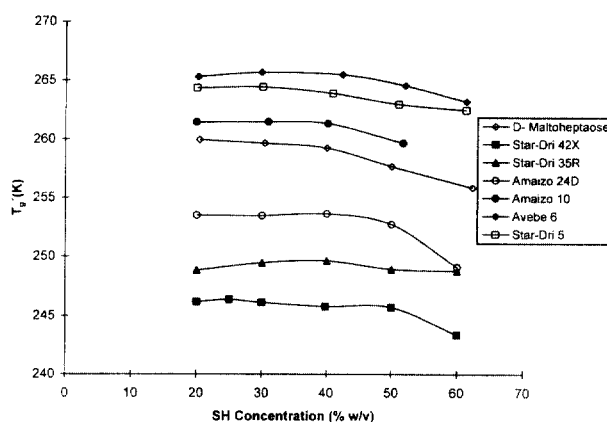


Fig. 3. Effect of solute concentration on  $T_g'$  of aqueous commercial starch hydrolysates.

stant heating rate during DSC, there were no substantial changes in  $T_g'$  with solute concentration, particularly in the range of 10–40% w/v. A slight decrease in  $T_g'$  was evident at higher solute concentrations. At high solute concentrations, increasing amounts of water are likely

to remain unfrozen when rapid cooling is employed, thus depressing further the apparent  $T_g'$  of the amorphous state. Indeed, for such SH solutions, exhibiting depressed  $T_g'$ , ice recrystallization (exothermic effect) was observed on the rewarming DSC traces, providing additional evidence for the non-equilibrium freezing of these samples.

According to Roos and Karel (1991d) and Ablett et al. (1992a,b) rapidly cooled solutions of small molecular weight carbohydrates are not at equilibrium. Thus, annealing of such samples under different temperature/time regimes would yield different values for  $T_g$  and  $T_g'$  on the rewarming DSC traces; e.g. annealing at temperatures between  $T_g$  and  $T_g'$  would result in elevation of the  $T_g$ , whereas annealing at temperatures close to or slightly above the  $T_g'$  would have a depressing effect on  $T_g$ , due to dilution of the glass by partial ice melting. Ablett et al. (1992a,b) have further demonstrated that true DSC estimates for the  $T_g'$  and the  $C_g'$  (of the maximally freeze-concentrated liquid phase) can be obtained only when an appropriate annealing protocol is adopted to permit maximum freeze-concentration in a frozen sample. These values should be used in constructing the phase diagram and identifying the intersection point between the equilibrium liquidus curve and the glass-transition curve. Without annealing of a rapidly cooled specimen, a  $T_g'$  determination from the immediate rewarming DSC curve (as done in the present study) does not necessarily provide a true estimate for  $T_g'$  of the maximally freeze-concentrated phase; i.e. it usually leads to an overestimation of the  $T_g'$ . Nevertheless, the apparent  $T_g'$  values, as obtained directly from the DSC heat-flow curves, denote the limit of mechanical stability in a practical time scale. According to Shalaev and Franks (1995), this transition temperature is of greater significance than the true glass transition temperature as it is related to the mechanical collapse of the amorphous matrix in real time, followed by phase separations and pronounced chemical deterioration of labile constituents.

A further aspect of the low temperature behavior of frozen carbohydrate solutions was to test the applicability of simple predictive models for estimating the  $T_g'$  of 'binary' mixtures of solutes (at constant solute concentration of 30% w/v) and even composite samples (e.g. the commercial SHs) based on the oligosaccharide composition and their respective  $T_g'$ . For the binary systems of either pure malto-oligosaccharides or blends of two SHs of known  $T_g'$  value, the relationship:

$$\frac{1}{T_g} = \frac{w_1}{T_{g1}} + \frac{w_2}{T_{g2}}$$

seemed to predict, fairly well, the  $T_g'$  of the frozen solutions (total solute concentration 30% w/v), regardless of the weight ratio between the two components

(Fig. 4). This rationale was further extended to poly-disperse systems using 24 SHs, whose oligosaccharide composition (determined by HPLC) is given in Table 1. Differences in oligosaccharide profiles were not only detected among samples of varying DE, but also among SHs of identical DE provided by different suppliers. Based on their composition and the experimentally determined values of  $T_g'$  for the pure malto-oligosaccharides, estimates of  $T_g'$  of the SHs were made using the generalized Flory–Fox equation, given in the Methods section. For the components with a DP > 7, an average value of  $T_g' \approx 261$  K was used for computation of  $T_g'$  for the SHs. A comparison of data for the predicted and experimentally determined  $T_g'$ s is presented in Fig. 5(a). Although a linear relationship between the two temperatures holds, there seems to be a deviation of the observed and the estimated  $T_g'$  values using the Flory–Fox equation, particularly for the high DE products; i.e. the predicted values are overestimates of the DSC-determined  $T_g'$ s. To examine the possibility of having greater free volume effects, due to the presence of branched oligosaccharides in the SHs, as is known for branched synthetic polymers and glucans (Bizot et al., 1997), the hydrolyzates were debranched with a purified pullulanase preparation; this enzyme hydrolyzes selectively  $\alpha$ -(1→6) linkages, converting the SH into a mixture of linear glucan chains. HPLC analysis of the debranched SHs revealed only minor changes in the oligosaccharide profiles (data not shown) of these samples. Once again, there was a linear relationship between  $T_g'$  predicted and  $T_g'$  measured for the composite glasses (Fig. 5(b)) in the frozen state. Moreover, a similar deviation to that of Fig. 5(a) was observed between the predicted and the calorimetric  $T_g'$  values for the debranched SHs. More information is needed on the low temperature behavior of such polydisperse carbohydrate solutions, in the supercooled and glassy state, to explain these trends.

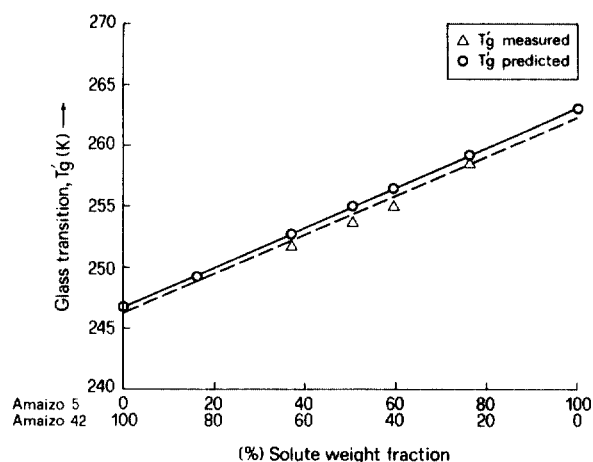


Fig. 4. Prediction of  $T_g'$  for binary mixtures (Amaizo 42/Amaizo 5); total solute concentration 30% (w/v).

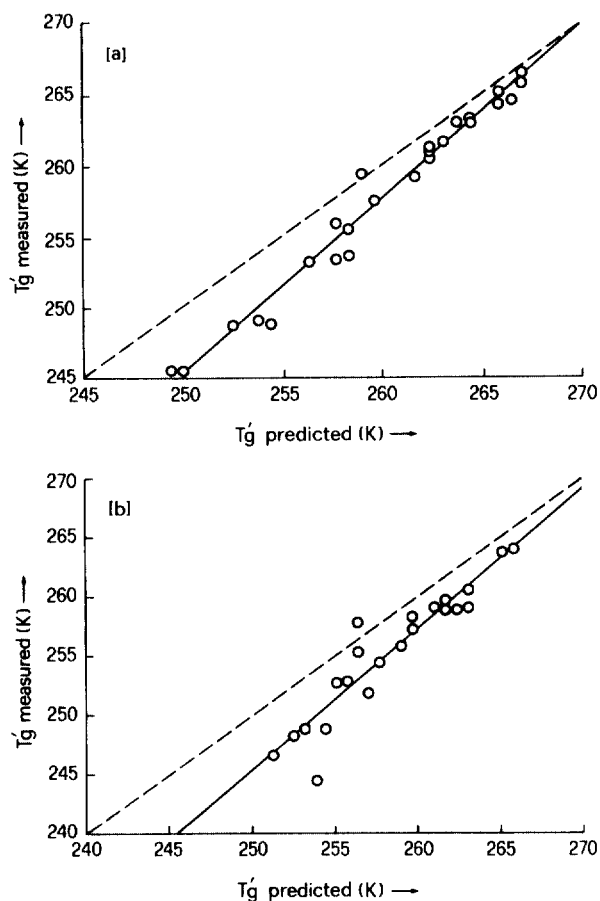


Fig. 5. Comparison between  $T_g'$  predicted (Flory–Fox equation) and  $T_g'$  measured (calorimetry) for commercial starch hydrolyzates (a) and pullulanase-debranched hydrolyzates (b).

### 3.2. Reaction kinetics in frozen SHs solutions

The main objective of numerous studies on low temperature behavior of model binary and ternary systems (solute(s)-water) has been to extrapolate the findings to more complex food systems. The overall cryostabilization framework of frozen food items, as developed and extensively discussed in several reviews by Levine and Slade (1988b, 1990) and Slade and Levine (1991), focuses on the ability to store the food at temperatures less than its  $T_g$  and/or modify the food formulation to increase its  $T_g$  to above normal storage temperature. Levine and Slade (1988b, 1990) have also promoted the idea of  $T_g'$  as being the threshold of instability in frozen foods, and that reaction kinetics above this boundary are controlled by the difference between the storage temperature and the specific  $T_g'$  of the product ( $\Delta T = T - T_g'$ ) according to the WLF kinetic theory. This relationship predicts a much stronger dependence of reaction kinetics on temperature than the Arrhenius equation. Knowing the influence of temperature on the kinetics of quality deterioration processes can be very critical when attempting to optimize storage protocols

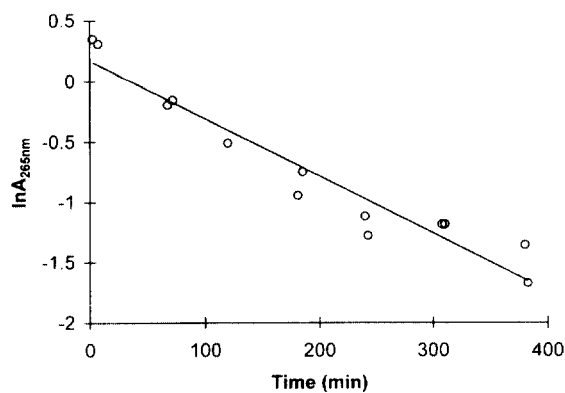


Fig. 6. Oxidation kinetics of ascorbic acid ( $2.5 \text{ mg ml}^{-1}$ ) in a frozen solution of Maltrin M150 (20% w/v in acetate buffer, 0.02 M, pH 5.5, containing 1500 ppm  $\text{H}_2\text{O}_2$ ) at  $-4^\circ\text{C}$ .

to improve the shelf-life of a product and minimize storage costs.

Simatos et al. (1989), analyzing various published data for frozen products, have concluded that the reaction rate constants in the temperature range of  $\sim T_g' < T < T_g' + 40^\circ\text{C}$  (the  $T_g'$  being defined according to Levine and Slade, 1986) were more weakly dependent on temperature than that predicted from a typical WLF response with the use of the 'universal' coefficients ( $C_1 = 17.44$  and  $C_2 = 51.6$ ). Among other reasons provided to explain such behavior were (Simatos et al.; Simatos & Blond, 1991; Karel & Saguy, 1991): (a) dissolution (melting) of ice above  $T_g'$  (i.e. dilution of reactants) could partly compensate the acceleration in reaction kinetics due to decreasing viscosity with increase in temperature; (b) reactant diffusivity (particularly for small molecular weight reactants) may not be as strongly dependent on temperature changes as assumed by the 'WLF formalism'; (c) food matrix composition and added solutes or solvents/diluents to modify the effective  $T_g'$  may also exert specific effects on reaction kinetics; (d) rates of some reactions may not be diffusion-limited and thus do not conform to WLF kinetics (Fennema, 1996); and (d) for frozen items, adoption of  $T_g$  as a reference temperature, rather than  $T_g'$ , may be more relevant for defining the operational WLF temperature domain.

In the present study we have examined the potential of SHs, used as modifiers of the glass transition temperature, for controlling the oxidation rate of ascorbic acid as a result of changes in the physical state of the concentrated solute matrix. The pH of the system and the ascorbic acid concentration were kept constant, hydrolyzates of varying DE were used, and  $\text{H}_2\text{O}_2$  was included to ensure oxygen availability (Hatley, 1986). In the presence of  $\text{O}_2$ , ascorbic acid is oxidized to dehydroascorbic acid. Using UV spectroscopy, the disappearance of the enediol can be followed (Fig. 6) and an apparent first-order reaction rate constant can be calculated. The rate constants are summarized in

Table 2  
Rate constants of ascorbic acid oxidation in frozen SH matrices

Sample	Rate constant, $k \times 10^2$ ( $\text{min}^{-1}$ )			
	$-16^\circ\text{C}$	$-12^\circ\text{C}$	$-8^\circ\text{C}$	$-4^\circ\text{C}$
Control (no SH added)	$2.06 \pm 0.10^a$	$2.53 \pm 0.29$	$2.83 \pm 0.29$	$2.95 \pm 0.65$
Star-Dri 42F (20%) <sup>b</sup>	$0.04 \pm 0.01$	$0.06 \pm 0.01$	$0.11 \pm 0.02$	$0.21 \pm 0.02$
Maltrin M365 (20%)	$0.04 \pm 0.01$	$0.09 \pm 0.01$	$0.16 \pm 0.04$	$0.41 \pm 0.07$
Maltrin M200 (20%)	$0.11 \pm 0.03$	$0.24 \pm 0.10$	$0.39 \pm 0.16$	$0.83 \pm 0.21$
Maltrin M150 (20%)	$0.15 \pm 0.01$	$0.29 \pm 0.06$	$0.53 \pm 0.16$	$0.94 \pm 0.28$
Star-Dri 42F (40%)	$0.01 \pm 0.00$	$0.03 \pm 0.01$	$0.08 \pm 0.03$	$0.25 \pm 0.11$
Maltrin M365 (40%)	$0.02 \pm 0.01$	$0.04 \pm 0.01$	$0.08 \pm 0.02$	$0.19 \pm 0.04$
Maltrin M200 (40%)	$0.05 \pm 0.02$	$0.08 \pm 0.02$	$0.32 \pm 0.13$	$0.77 \pm 0.22$
Maltrin M150 (40%)	$0.05 \pm 0.02$	$0.10 \pm 0.03$	$0.28 \pm 0.03$	$0.48 \pm 0.12$

<sup>a</sup> Data represent means of at least duplicate experiments  $\pm$  SD.

<sup>b</sup>  $k$  Values determined using a first-order reaction model.

Table 2. The measured  $k$  values for the control samples were in reasonable agreement with the data of Hatley et al. (1986); these authors have reported a rate of  $\sim 1.79 \times 10^{-2} \text{ min}^{-1}$  at  $-20^\circ\text{C}$  for oxidation of ascorbic acid solutions with a concentration of 1.7 mg/100 ml. The rate constants for the SH-containing solutions (Table 2) were significantly lower than those of the control sample (with no additives). Moreover, the more concentrated samples (40% w/v SH) had lower reaction rates than the dilute preparations. One interesting observation was that, at each storage temperature tested, the reaction rate increased with decreasing DE of the SH matrix. This behavior was not anticipated considering the inverse relationship between  $T_g'$  and DE. Similar observations were also made by Lim and Reid (1991) when examining the cryostabilization potential of a maltodextrin sample (DE 10; at 10% w/v) and CMC (having at least as high  $T_g'$  as the maltodextrin). Their results indicated that CMC was not effective in controlling the rate of ascorbic acid oxidation compared to the maltodextrin matrix. They have thus concluded that, knowing only the  $T_g'$  of a water soluble polymer is not sufficient to predict its cryostabilization effectiveness when added in a frozen food formulation. On the other hand, for an enzymic hydrolysis reaction, the same authors have found increasing rates in frozen maltodextrin solutions (at  $T > T_g'$ ) with increasing DE. At this stage, mention must be made that, with multi-component reaction mixtures, as those of the frozen SHs–ascorbic acid– $\text{O}_2$ , where the reactive species differ widely in their molar volumes, it is unlikely that diffusion of small molecules (e.g.  $\text{O}_2$ ) within the amorphous matrix is controlled by similar motional constraints as the maltodextrin molecules around their glass transition region; i.e. small molecules would not experience the same glass transition as the matrix.

The effect of storage temperature on reaction kinetics was examined by both the Arrhenius (Fig. 7) and the WLF (Fig. 8) equations. Estimates of the activation

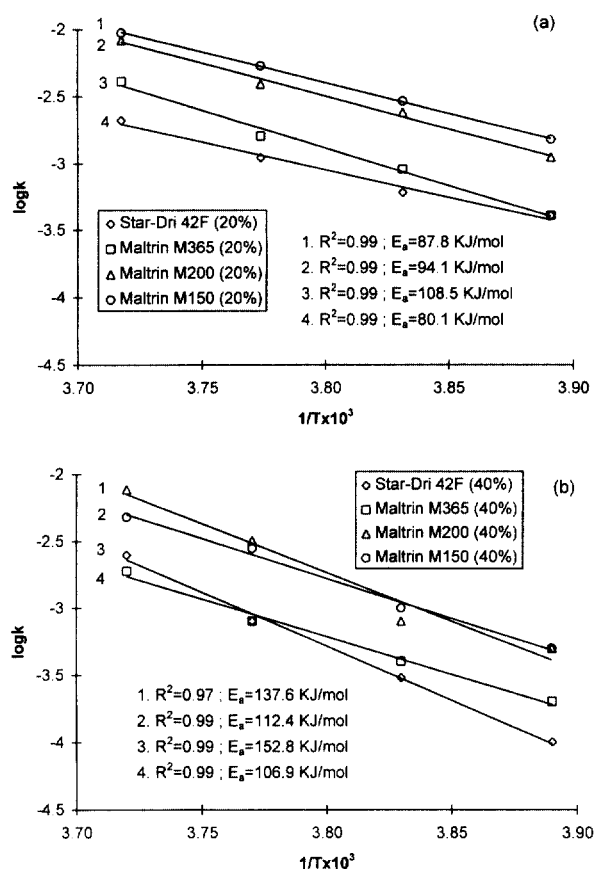


Fig. 7. Arrhenius plots for first-order reaction rate constants of ascorbic acid oxidation in frozen commercial maltodextrin solutions.

energies ( $E_a$ ) from the Arrhenius model ranged generally between 80 and 150  $\text{kJ mol}^{-1}$ . These values are consistent with an average value of  $\sim 125 \text{ kJ mol}^{-1}$  reported for nutrient losses and non-enzymic reactions in foods (Taoukis & Labuza, 1996) as well as the range of 100–170  $\text{kJ mol}^{-1}$  for ascorbic acid oxidation in frozen vegetables and fruit (Guadagni & Kelly, 1958; Kramer, 1974). It was of interest to note that fairly



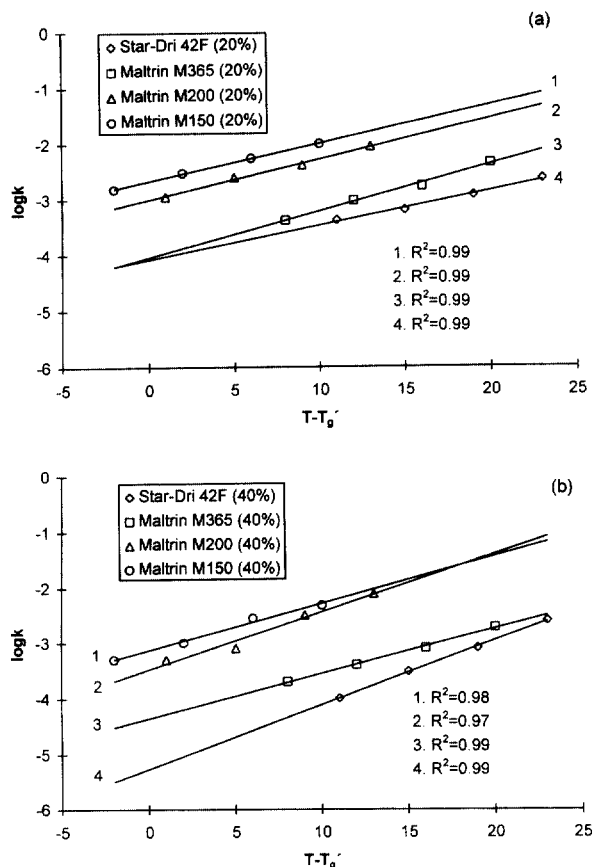


Fig. 8. WLF (Williams–Landel–Ferry) plots for first-order reaction rate constants of ascorbic acid oxidation in frozen commercial maltodextrin solutions.

good fits were obtained for all data using both kinetic models. This was somewhat surprising considering the arguments put by Simatos et al. (1989) and Simatos and Blond (1991) for the deviation between the WLF and the Arrhenius-type dependence of reaction rates in frozen food products. A possible explanation for this behavior may be the relatively narrow temperature range, above the  $T_{ref}$  ( $T_g'$ ) for each system, over which testing of the two models was carried out. Nevertheless, it is obvious from these plots that in the temperature range of industrial frozen storage, and for a span of  $\Delta T = T - T_g' \approx 12^\circ\text{C}$ , both the WLF and the Arrhenius equations can be used to describe, reasonably well, the temperature dependence of reaction rates of ascorbic acid oxidation in model frozen systems. Peleg (1992) has suggested that the applicability of the WLF kinetic model and its validity with fixed 'universal' constants should be verified over a large temperature range for each particular system. Finally, the most important point one can make from the results of Table 2 is that the  $T_g'$  of the freeze-concentrated maltodextrin matrix, by itself, may not necessarily be helpful in determining the stability of the system during frozen storage.

## References

- Ablett, S., Izzard, M. J., & Lillford, P. J. (1992a). Differential scanning calorimetric study of frozen sucrose and glycerol solutions. *J. Chem. Soc. Faraday Trans.*, *88*, 789–794.
- Ablett, S., Clark, A. H., Izzard, M., & Lillford, P. J. (1992b). Modelling of heat capacity–temperature data for sucrose–water systems. *J. Chem. Soc. Faraday Trans.*, *88*, 795–802.
- Bizot, H., Le Bail, P., Leroux, B., Davy, J., Roger, P., & Buleon, A. (1997). Calorimetric evaluation of the glass transition in hydrated, linear and branched polyhydroglucose compounds. *Carbohydr. Polym.*, *32*, 33–50.
- Blond, G. (1989). Water–galactose system: supplemented state diagram and unfrozen water. *Cryo-Lett.*, *10*, 299–308.
- Blond, G., & Simatos, D. (1991). Glass transition of the amorphous phase in frozen aqueous systems. *Thermochim. Acta*, *175*, 239–247.
- Fennema, O. R. (1996). Water and ice. In: O. R. Fennema (Ed.), *Food chemistry* 3rd ed., (pp. 18–88). New York: Marcel Dekker.
- Ferry, J. D. (1980). *Viscoelastic properties of polymers* 3rd ed. New York: John Wiley & Sons.
- Fox, T. G., & Flory, P. J. (1950). Second-order transition temperatures and related properties of polystyrene. *J. Appl. Phys.*, *21*, 581–591.
- Fox, T. G., & Flory, P. J. (1954). *J. Polym. Sci.* *14*, 315; as cited in Fuzek, J. (1980). Glass transition temperature of wet fibers. In *Water in polymers*, S. Powland (Ed.), ACS Symposium Series (Vol. 127, pp. 515–530). Washington, DC: American Chemical Society.
- Guadagni, D. G., & Kelly, S. H. (1958). Time–temperature tolerance of frozen foods. XIV. Ascorbic acid and its oxidation products as a measure of temperature history in frozen strawberries. *Food Technol.*, *12*, 645–647.
- Hatley, H. M., Franks, F., & Day, H. (1986). Subzero-temperature preservation of reactive fluids in the undercooled state. II. The effect on the oxidation of ascorbic acid of freeze concentration and undercooling. *Biophys. Chem.*, *24*, 187–192.
- Karel, M., & Saguy, I. (1991). Effect of water on diffusion in food systems. In H. Levine & L. Slade (Eds.), *Water relationships in foods* (pp. 157–173). New York: Plenum Press.
- Kramer, A. (1974). Storage retention of nutrients. *Food Technol.*, *28*(1), 50–60.
- Levine, H., & Slade, L. (1986). A polymer physicochemical approach to the study of commercial starch hydrolysis products (SHPs). *Carbohydr. Polym.*, *6*, 213–244.
- Levine, H., & Slade, L. (1988a). Thermomechanical properties of small-carbohydrate glasses and "rubbers". Kinetically metastable systems at sub-zero temperatures. *J. Chem. Soc. Faraday Trans. 1*, *84*, 2619–2633.
- Levine, H., & Slade, L. (1988b). Principles of cryo-stabilization technology from structure/property relationships of carbohydrate/water systems. *Cryo-Lett.*, *9*, 21–63.
- Levine, H., & Slade, L. (1988c). Water as a plasticizer: physico-chemical aspects of low-moisture polymeric systems. In F. Franks (Ed.), *Water science reviews* (Vol. 3, pp. 79–185). Cambridge: Cambridge University Press.
- Levine, H., & Slade, L. (1990). Cryostabilization technology: thermo-analytical evaluation of food ingredients and systems. In V. R. Harwalker & C. Y. Ma, E. (Eds.), *Thermal analysis of foods* (pp. 221–303). New York: Elsevier Applied Science.
- Lim, M. H., & Reid, D. S. (1991). Studies of reaction kinetics in relation to the  $T_g'$  of polymers in frozen model systems. In H. Levine & L. Slade (Eds.), *Water relationships in foods* (pp. 103–122). New York: Plenum Press.
- Mansfield, M. (1993). An overview of theories of the glass transition. In J. M. V. Blanshard & P. J. Lillford (Eds.), *The glassy state in foods* (pp. 103–122). Loughborough, UK: Nottingham University Press.
- Orford, P. D., Parker, R., Ring, S. G., & Smith, A. C. (1989). Effect of water as a diluent on the glass transition behaviour of

- malto-oligosaccharides, amylose and amylopectin. *Int. J. Biol. Macromol.*, *11*, 91–96.
- Peleg, M. (1992). On the use of the WLF model in polymers and foods. *Crit. Rev. Food Sci. Nutr.*, *32*, 59–66.
- Racker, E. (1952). Spectrophotometric measurements of the metabolic formation and degradation of thiol esters and enediol compounds. *Biochem. Biophys. Acta*, *9*, 577–578.
- Roos, Y., & Karel, M. (1991). Phase transitions of amorphous sucrose and frozen sucrose solutions. *J. Food Sci.*, *56*, 266–267.
- Roos, Y., & Karel, M. (1991). Water and molecular weight effects on glass transitions in amorphous carbohydrates and carbohydrate solutions. *J. Food Sci.*, *56*, 1676–1681.
- Roos, Y., & Karel, M. (1991). Nonequilibrium ice formation in carbohydrate solutions. *Cryo-Lett.*, *12*, 367–376.
- Roos, Y., & Karel, M. (1991). Amorphous state and delayed ice formation in sucrose solutions. *Int. J. Food Sci. Technol.*, *26*, 553–566.
- Roos, Y. (1995). Characterization of food polymers using state diagrams. *J. Food Eng.*, *24*, 339–360.
- Shalaev, E. Y., & Franks, F. (1995). Structural glass transitions and thermophysical processes in amorphous carbohydrates and their supersaturated solutions. *J. Chem. Soc. Faraday Trans.*, *91*, 1511–1517.
- Simatos, D., Blond, G., & Le Meste, M. (1989). Relation between glass transition and stability of a frozen product. *Cryo-Lett.*, *10*, 77–84.
- Simatos, D., & Blond, G. (1991). DSC studies and stability of frozen foods. In H. Levine & L. Slade (Eds.), *Water relationships in foods* (pp. 139–155). New York: Plenum Press.
- Slade, L., & Levine, H. (1991). Beyond water activity: recent advances based on an alternative approach to the assessment of food quality and safety. *Crit. Rev. Food Sci. Nutr.*, *30*, 115–360.
- Slade, L., & Levine, H. (1994). Water and the glass transition—dependence of the glass transition on composition and chemical structure: special implications for flour functionality in cookie baking. *J. Food Eng.*, *22*, 143–188.
- Taoukis, P., & Labuza, T. (1996). Integrative concepts in food. In O. R. Fennema (Ed.), *Food chemistry* (3rd ed., pp. 1013–1039). New York: Marcel Dekker.
- To, E. C., & Flink, J. M. (1978). “Collapse”, a structural transition in freeze dried carbohydrates. II. Effect of solute composition. *J. Food Technol.*, *13*, 567–581.
- Wasylyk, J. M., & Baust, J. G. (1991). Vitreous domains in an aqueous ribose solution. In H. Levine & S. Slade (Eds.), *Water relationships in foods* (pp. 225–234). New York: Plenum Press.
- Williams, M. L., Landel, R. F., & Ferry, J. D. (1955). The temperature dependence of relaxation mechanisms in amorphous polymers and other glass-forming liquids. *J. Am. Chem. Soc.*, *77*, 3701–3707.